frontiers in Immunology

METHODS
published: 08 August 2018
doi: 10.3389/fimmu.2018.01840

Single-Fluorescent Protein Reporters Allow Parallel Quantification of Natural Killer Cell-Mediated Granzyme and Caspase Activities in Single Target Cells

Clarissa Liesche[1], Patricia Sauer[1], Isabel Prager[2], Doris Urlaub[2], Maren Claus[2], Roland Eils[1], Joël Beaudouin[1] and Carsten Watzl[2]**

[1] Division of Theoretical Bioinformatics at German Cancer Research Center (DKFZ), Department for Bioinformatics and Functional Genomics, Institute for Pharmacy and Molecular Biotechnology, BioQuant Center, Heidelberg University, Heidelberg, Germany, [2] Department for Immunology, Leibniz Research Centre for Working Environment and Human Factors at TU Dortmund (IfADo), Dortmund, Germany

OPEN ACCESS

Edited by:
Eric O. Long,
National Institute of Allergy and Infectious Diseases (NIAID), United States

Reviewed by:
Emily Mace,
Columbia University, United States
Konrad Krzewski,
National Institute of Allergy and Infectious Diseases (NIAID), United States

***Correspondence:**
Joël Beaudouin
joel.beaudouin@ibs.fr;
Carsten Watzl
watzl@ifado.de

Specialty section:
This article was submitted to NK and Innate Lymphoid Cell Biology, a section of the journal Frontiers in Immunology

Received: 05 June 2018
Accepted: 25 July 2018
Published: 08 August 2018

Citation:
Liesche C, Sauer P, Prager I, Urlaub D, Claus M, Eils R, Beaudouin J and Watzl C (2018) Single-Fluorescent Protein Reporters Allow Parallel Quantification of Natural Killer Cell-Mediated Granzyme and Caspase Activities in Single Target Cells. Front. Immunol. 9:1840. doi: 10.3389/fimmu.2018.01840

Natural killer (NK) cells eliminate infected and tumorigenic cells through delivery of granzymes *via* perforin pores or by activation of caspases *via* death receptors. In order to understand how NK cells combine different cell death mechanisms, it is important to quantify target cell responses on a single cell level. However, currently existing reporters do not allow the measurement of several protease activities inside the same cell. Here, we present a strategy for the comparison of two different proteases at a time inside individual target cells upon engagement by NK cells. We developed single-fluorescent protein reporters containing the RIEAD or the VGPD cleavage site for the measurement of granzyme B activity. We show that these two granzyme B reporters can be applied in combination with caspase-8 or caspase-3 reporters. While we did not find that caspase-8 was activated by granzyme B, our method revealed that caspase-3 activity follows granzyme B activity with a delay of about 6 min. Finally, we illustrate the comparison of several different reporters for granzyme A, M, K, and H. The approach presented here is a valuable means for the investigation of the temporal evolution of cell death mediated by cytotoxic lymphocytes.

Keywords: natural killer cells, cytotoxic lymphocytes, single-fluorescent protein reporters, granzyme and caspase activity, apoptosis and cell death

INTRODUCTION

As part of the innate immune system, natural killer (NK) cells can eliminate infected and tumorigenic cells (1). To do so, they adhere to a target cell and establish an immunological synapse (2). The following NK cell receptor signaling can trigger the release of cytotoxic granules from the NK cell into the cleft of this synapse (3). Like cytotoxic T lymphocytes (CTLs), NK cells have two mechanisms to induce cell death of target cells. In the first mechanism, granzymes are released from cytotoxic granules and enter the target cell *via* perforin pores and induce cell death. In the second mechanism, CD95L or TRAIL are presented at the surface of NK cells and induce extrinsic apoptosis in target cells through activation of the death receptors CD95 or TRAIL-R1/-R2 (4, 5).

How NK cells orchestrate the activities of granzymes and the activation of extrinsic apoptosis remains poorly understood. Extrinsic apoptosis starts with the formation of the so-called death-inducing signaling complex, composed of activated death receptors and recruited FADD adaptor proteins and initiator procaspases-8/-10. Once activated, these caspases cleave and activate effector procaspase-3/-7 (6, 7), leading to apoptosis, unless presence of XIAP blocks their activity (8, 9). When the pro-apoptotic Bcl-2 protein BID is cleaved by caspase-8/-10 in sufficient amount, truncated BID induces mitochondrial outer membrane permeabilization. Subsequent release of cytochrome c activates caspase-9, while release of SMAC induces the degradation of XIAP, both leading to massive activation of effector caspases.

To deliver granzymes in the cytosol of target cells, perforin forms a pore in cellular membranes (10). It is debated if this occurs at the plasma membrane (11, 12) or the membrane of endosomes (13–15). Of the five human granzymes A, B, H, K, and M, granzyme B is the best characterized one and shares substrate specificity with caspases for cleavage after aspartate residues (16–18). Both, granzyme B and caspase-8 can cleave BID, yet, at different sites, at D75 (RIEAD'S) and D60 (ELQTD'G) (19), respectively. While granzyme B has been shown to cleave the initiator procaspase-8 (20) and the effector procaspase-3 (21–25), other substrates measured *in vitro* have been reported to be more efficiently cleaved, for example, DNA-PKc or BID (23, 26–28). From this perspective, granzyme B is suggested to play a role not only as an initiator but also as executioner enzyme in target cell death (9).

Having reporters that would allow the measurement of the contribution of granzymes and caspases in a single cell would be beneficial to characterize the activity of NK cells. Specific protease biosensors based on luciferase (29, 30), fluorophore quenching (31), and FRET (32, 33) (**Table 1**) have facilitated the study of the killing mechanism by granzymes and death receptors. However, they do not easily allow multiplexing for the quantification of several protease activities in single cells. Parallel assessment of protease activity inside single cells would allow for a better understanding of the temporal order of signaling events in the NK cell killing mechanism. In order to reach this aim, we present an approach to measure NK cell-mediated activity of two proteases at once in single target cells. We demonstrate our approach by measuring granzyme B, caspase-8, and caspase-3 activity in target cells exposed to NK cells. The pallet of reporters can easily be extended by cloning cleavage linkers, as illustrated here with the measurement of potential substrates for different granzymes. We believe that these reporters offer a valuable resource to characterize the physiology of NK cells or to test the activity of patient-derived NK cells.

TABLE 1 | Cleavage sites used in this study.

Substrate/ cleavage site	Cleaved by protease	Protein containing the cleavage site	Reference
ELQTD'G	Caspase-8/-10	Human BID	(19, 34)
RIEAD'S	Granzyme B, Caspase-10	Human BID	(19, 29, 35–37)
DEVD'R	Caspase-3/-7	PARP-1	(29, 38)
VGPD'FGR	Granzyme B	DNA-PK	(29, 31–33, 35)
RIEPD'S	Granzyme B	Mouse BID	(36, 39)
IGNR'S	Granzyme A		(39)
PTSY'G	Granzyme H		(39)
YRFK'G	Granzyme K		(39, 40)
KVPL'AA	Granzyme M		(39, 41)
DVAHK'QL	Granzyme A	NDUFS3	(42)

RESULTS

Measurement of Protease Activity Induced by NK Cells in Living Target Cells

To get insights into the process by which individual NK cells kill their target cells, we aimed at comparing the strength of different proteases inside single target cells. To achieve this, we designed fluorescent reporters following the strategy that we previously established to measure caspase activity upon CD95 activation (34). These reporters consist of one fluorescent protein fused to a localization domain through a linker that can be specifically cleaved by proteases. In this study, we use the nuclear export signal (NES) as localization domain (**Figure 1**). As exemplified below, this reporter allows an easy quantification of protease activity, and it detects any activity originating from an enzyme facing the cytosol. Protease cleavage leads to separation of the fluorescent protein from the localization domain. The free fluorescent protein is small enough to enter or exit the nucleus by passive diffusion, a process that takes about 1 min. Reporter cleavage can be quantified by measuring the increase of fluorescence signal in the nucleus. This is ideally imaged by time-lapse fluorescence confocal microscopy as this allows the measurement of the fluorescence intensity inside the nucleus without contamination of signal from the cytosol below and above. Thus, by quantifying the spatial redistribution of the fluorescence signal inside the target cell, reporter cleavage can be calculated. Image analysis can be done using the freely available ImageJ software and proceeds as follows: generation of an image stack from time series data, background subtraction, and measurement of the mean fluorescence signal in a region of interest representing the cell nucleus. To estimate the extent of substrate cleavage, this nuclear signal is normalized to the

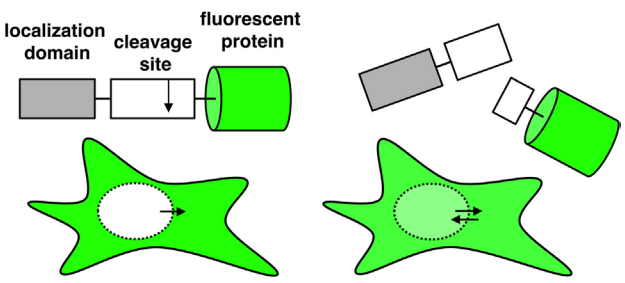

FIGURE 1 | Schematic representation of a single-fluorescent protein (single FP) reporter and its fluorescence distribution inside the cell when using a nuclear export signal as localization domain. Upon cleavage of the reporter, the fluorescent protein can diffuse passively into the nucleus.

cytosolic one. One possibility is to perform this normalization for each time point, which requires more work but has the advantage of correcting for potential photobleaching over time:

$$I_{\text{nucleus}}^{\text{normalized}}(t) = \frac{I_{\text{nucleus}}(t)}{I_{\text{cytosol}}(t)}$$

In this case, the normalized intensity tends toward 1, or 100%, when cleavage is complete. The data presented here were analyzed in this way. The second possibility consists of normalizing with the cytosolic signal before the addition of the NK cells. This approach is relevant if photobleaching can be neglected:

$$I_{\text{nucleus}}^{\text{normalized}}(t) = \frac{I_{\text{nucleus}}(t)}{I_{\text{cytosol}}(t=0)}$$

In this case, as the nucleus and the cytoplasm are roughly occupying the same volume, the normalized intensity tends toward 0.5 or 50%.

Since each reporter contains only one fluorescent protein, these so-called single-fluorescent protein reporters allow parallel assessment of several reporters within the same cell. Hence, different comparison can be realized: the measurement of (i) different cleavage sites for different proteases or of (ii) different cleavage sites for the same protease.

Granzyme B Activity Can Be Measured With Single-Fluorescent Protein Reporters Having the RIEADS or the VGPD Cleavage Site

In order to establish single-fluorescent protein reporters for the measurement of granzyme B activity, we designed and tested two different reporters carrying a linker sequence known to be cleaved by granzyme B. The first reporter carries the amino acid sequence RIEADS (single amino acid code), which is present in the protein BID. The second reporter carries the amino acid sequence VGPD from the protein DNA-PKc as cleavable linker. We co-expressed the two reporters NES-RIEADS-mCherry and NES-VGPD-mGFP in HeLa cells expressing CD48, a ligand for the activating NK cell receptor 2B4 (CD244), which renders them more sensitive to killing by NK cells (43). The transfected target cells were imaged by confocal laser scanning microscopy over time upon addition of the human NK cell line NK92-C1. Cell death was recognized from images by cell rounding and cell shrinkage following NK cell engagement (**Figure 2A**). About 20 min before target cell death, NES-RIEADS-mCherry and NES-VGPD-mGFP reporter cleavage was detected from the appearance of fluorescence inside the nucleus (**Figure 2A**). In order to plot the cleavage kinetics of several cells independently of the time of NK cell engagement, we defined the time of death as time point 0. In this way, we found that both reporters were cleaved on average at the same rate before target cell death (**Figure 2B**). Furthermore, the cleavage efficiency of NES-RIEADS-mCherry and NES-VGPD-mGFP reporters inside the same cell correlated well, showing that both reporters are able to mirror the observed cell-to-cell variability of granzyme B activity (**Figure 2B**). We next verified the specificity of these two reporters by measuring their cleavage in cells that overexpress serpin B9, a natural inhibitor of granzyme B (44). Compared to control cells, the time of cell death was delayed in serpin B9 overexpressing cells (**Figures 2C,D**). Consistent with that, reporter cleavage was reduced from 53 to 17% (NES-RIEADS-mCherry) and from 34 to 6% (NES-VGPD-mCherry), showing that both reporters are suitable for the specific measurement of granzyme B activity.

Single-Fluorescent Protein Reporters Allow Multiplexing: Distinguishing Different Proteases Inside the Same Cell

CD95 signaling in HeLa cells leads to notable caspase-8 and -3 activation (34). On the one hand, it was reported that caspase-8 can get activated through cleavage by granzyme B (20). On the other hand, it was shown that granzyme B activates effector caspases through cleavage of BID (24, 25, 27, 28). Deciphering the contribution of caspase-8 and granzyme B to NK cell-mediated cell death, and in particular, the potential activation of caspase-8 by granzyme B, is an intriguing question that could help to better understand cell death signaling by NK cells.

Therefore, we tested if caspase-8 and granzyme B activity can be distinguished within the same cell using our single-fluorescent protein reporters. For this aim, we measured NES-ELQTD-mGFP (for caspase-8), together with either NES-RIEADS-mCherry or NES-VGPD-mCherry (for granzyme B). Upon addition of soluble trimerized CD95L (IZsCD95L) to HeLa cells, we observed efficient cleavage of the caspase-8 reporter NES-ELQTD-mGFP. In contrast, in the same cells, the NES-RIEADS-mCherry reporter was cleaved only up to 10% (**Figure 3A**) and the NES-VGPD-mCherry reporter was virtually not cleaved (**Figure 3B**). This shows that granzyme B activity (using either the RIEADS- or the VGPD-reporter) can be clearly distinguished from caspase-8 activity (using the ELQTD-reporter) within the same cell.

Transient expression of shRNA against CD95 led to a reduction of CD95 protein expression on the surface of HeLa cells (Figure S1 in Supplementary Material) and furthermore to absence of cell death and caspase-8 activity in a control experiment using IZsCD95L as inducer (**Figure 4A**). The nuclear protein H2B-eBFP2 served as a fluorescent marker to recognize cells that contain the plasmid encoding shRNA (**Figure 4B**). Upon addition of NK cells to HeLa (CD48) cells expressing control shRNA, we observed NES-RIEADS-mCherry reporter cleavage as expected indicating granzyme B activity. In addition, the NES-ELQTD-mGFP reporter was cleaved on average up to 7% indicating an additional activation of caspase-8 (**Figure 4C**). This caspase-8 activity could be due to the activation of caspase-8 by granzyme B, or due to the activation of death receptors during the engagement by the NK cells. To distinguish these two possibilities, we repeated the experiment in HeLa cells expressing a shRNA against CD95. The absence of CD95 expression abolished NES-ELQTD-mGFP reporter cleavage (**Figure 4D**). This demonstrates that the caspase-8 activity was due to activation of the CD95 pathway by NK cells, and it also reveals that caspase-8 is not, or not efficiently, activated by granzyme B. When using activated primary human NK cells as effectors,

we saw a similar cleavage of the NES-VGPD-mCherry granzyme B reporter and of the NES-ELQTD-mGFP caspase-8 reporter in HeLa cells and in MDA-MB-468 breast carcinoma cells (Figure S1 in Supplementary Material). This demonstrates that NK cells use granzyme B dependent (*via* cytotoxic granules) and caspase-8-dependent (*via* CD95) pathways to kill target cells.

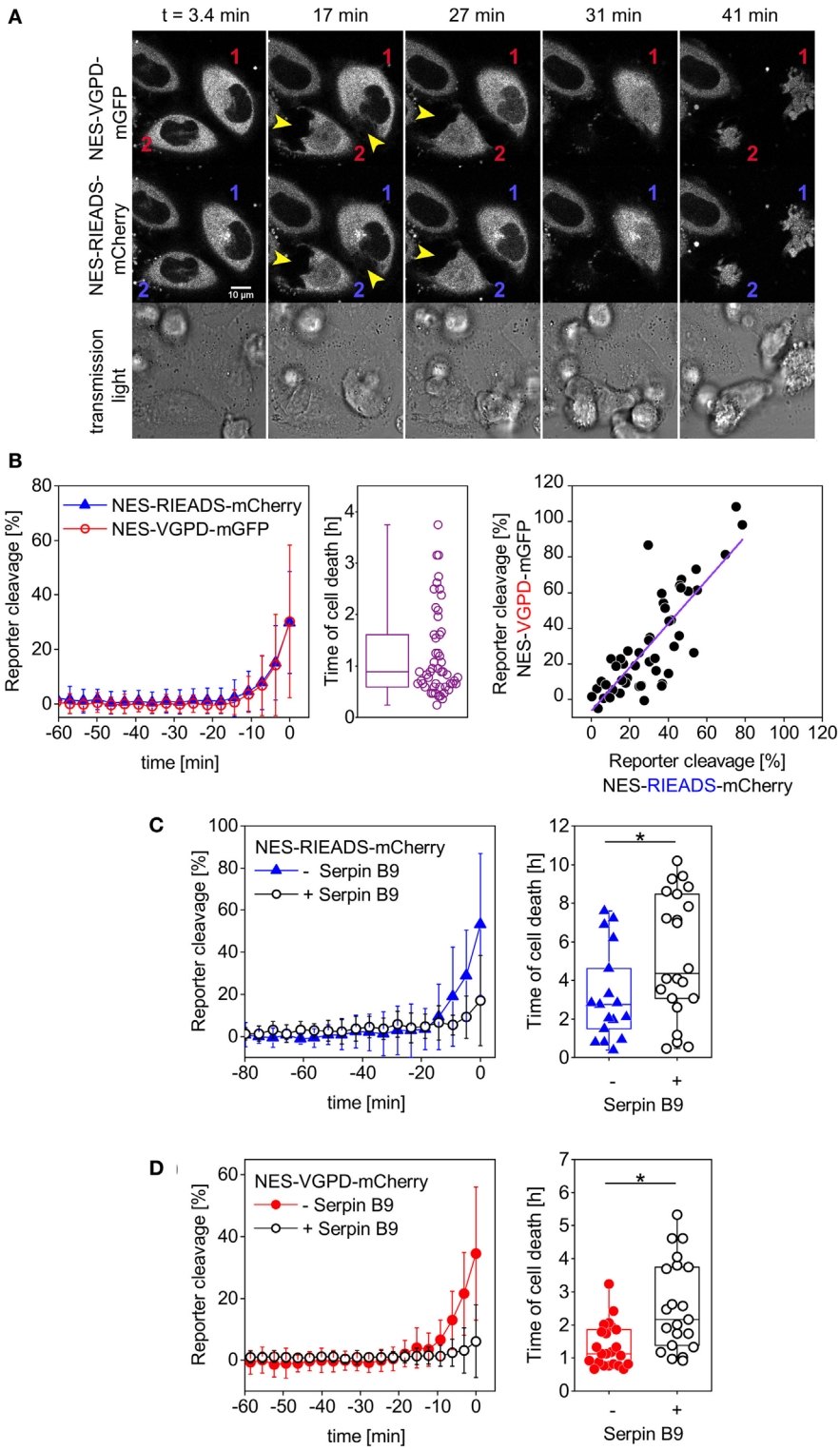

FIGURE 2 | Continued

FIGURE 2 | Measurement of granzyme B activity in target cells using single FP-reporters. **(A,B)** HeLa cells transfected with CD48, NES-VGPD-mGFP, and NES-RIEADS-mCherry were imaged by confocal microscopy upon incubation with threefold more NK92-C1 cells than target cells. **(A)** Representative images from confocal microscopy. Two target cells were labeled 1 and 2. Their contact with natural killer cells can be seen on fluorescence images (arrowheads). Appearance of fluorescence signal in the nucleus shows reporter cleavage. **(B)** NES-VGPD-mGFP and NES-RIEADS-mCherry reporter cleavage quantification. The last measurement point preceding cell death was set to time = 0 in order to calculate the mean and SD from 51 single cell measurements as shown. The boxplot shows the time of cell death of each cell. The scatter plot shows the correlation between NES-VGPD-mGFP and NES-RIEADS-mCherry reporter cleavage. Values correspond to the measurement point preceding cell death. Linear fit of data with slope = 1.23 ± 0.12 and Pearson's correlation coefficient = 0.82. **(C,D)** SerpinB9 expression in target cells reduces NES-VGPD-mCherry and NES-RIEADS-mCherry reporter cleavage induced by NK92-C1 cells. **(C)** HeLa (CD48) cells were transfected with NES-RIEADS-mCherry reporter alone or with the NES-RIEADS-mCherry reporter and serpin B9, E:T ratio = 1. Mean and SD of 17 and 22 cells, respectively. **(D)** HeLa (CD48) cells were transfected with NES-VGPD-mCherry reporter alone or with the NES-VGPD-mCherry reporter and serpin B9, E:T ratio = 3. Mean and SD of 23 and 22 cells, respectively. For cell death times shown in boxplots **(C,D)**, the mean between the control group and the test group (cells transfected with serpinB9) is significantly different at the 0.05 level.

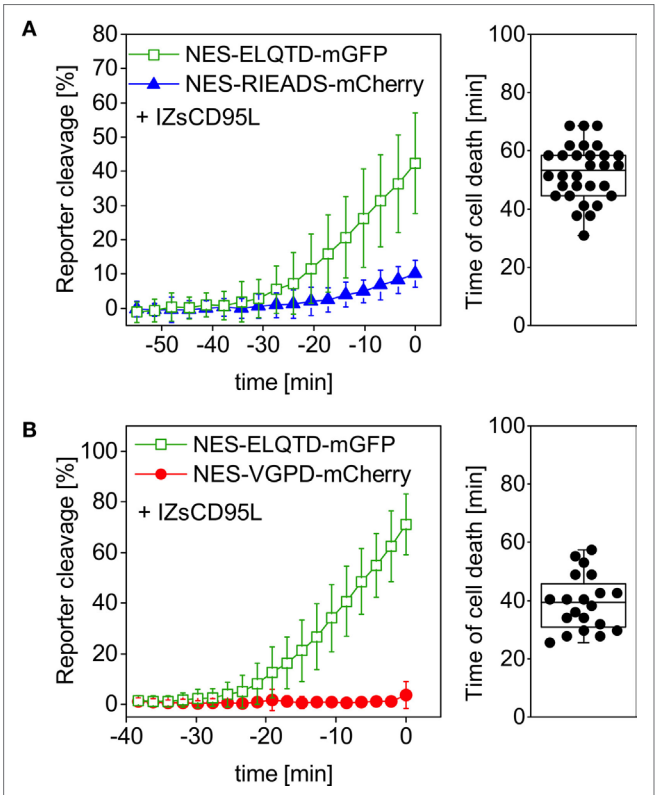

FIGURE 3 | Granzyme B activity can be distinguished from caspase-8 activity. HeLa cells overexpressing CD95 were transfected with **(A)** NES-ELQTD-mGFP (for caspase-8), and NES-RIEADS-mCherry for granzyme B or **(B)** NES-ELQTD-mGFP for caspase-8 and NES-VGPD-mCherry for granzyme B and imaged by confocal microscopy upon incubation with 1 µg/ml IZsCD95L.

It is known that effector caspase-3 activation can be a consequence of granzyme B activity (26). We thus hypothesized that caspase-3 activity should occur with a delay after granzyme B activity, as in the case of CD95-mediated extrinsic apoptosis (7, 34). To test this, we measured reporter cleavage of NES-VGPD-mCherry for granzyme B and NES-DEVDR-GFP for caspase-3 in HeLa cells upon addition of NK cells (**Figure 5A**). We found that caspase-3 activity appears on average about 6 min later than granzyme B (**Figure 5B**). The onset of caspase-3 activity was about 10 min before cell death, highlighting the speed of this cellular process. These data also show how precisely cell death can be analyzed on the single cell level with this approach using single-fluorescent protein reporters.

Testing Potential Reporters for Different Granzymes

Natural killer cells notably express granzyme A and B (45, 46), but they also express the less characterized granzymes H, K, and M (47). In order to further illustrate our approach and to potentially capture the activity of granzymes A, M, H, and K in single target cells, we designed fluorescent reporters that contain cleavage site candidates based on existing data from literature (**Table 1**). Using positional scanning combinatorial libraries, optimal substrates for the five human granzymes have been previously identified and characterized (39). Among them, the IEPD and IGNR sequence have been further developed as fluorescent label and inhibitor for granzyme B and granzyme A (39). Moreover, optimal substrates were determined to be YRFK for granzyme K, KVPL for granzyme M, and PTSY for granzyme H (39). In this study, we additionally designed a reporter containing the sequence DVAHKQL, which is present in the mitochondrial complex I protein NDUFS3, since granzyme A was reported to cleave this protein at this site after the amino acid lysine in this sequence (42). We measured these six different reporters in comparison to the granzyme B reporters NES-VGPD-mCherry or NES-RIEADS-mGFP. We found that the RIEADS and VGPD reporters were more sensitive to detect granzyme B activity compared to the IEDP reporter (**Figure 6A**). Also, granzyme B activity was clearly dominant among the different experiments as at the time of death IGNRS (granzyme A), PTSYG (granzyme H), and YRFKG (granzyme K) reporter cleavage was in almost all cases less than RIEADS or VGPD (granzyme B) cleavage (**Figure 6**). Moreover, no cleavage of DVAHQL (granzyme A) and KVPL (granzyme M) reporters could be observed. This comparison of different reporters would suggest that granzyme B and granzyme A are the most abundant granzymes used by the NK92-C1 to cleave substrates in the cytosol of target cells. This experiment shows how single-fluorescent protein reporter can be used to examine protease activity that is either induced inside target cells or stemming from cytotoxic lymphocytes such as NK cells.

DISCUSSION

The single-fluorescent protein reporters employed in this study are part of a larger panel of protease reporters, based, for

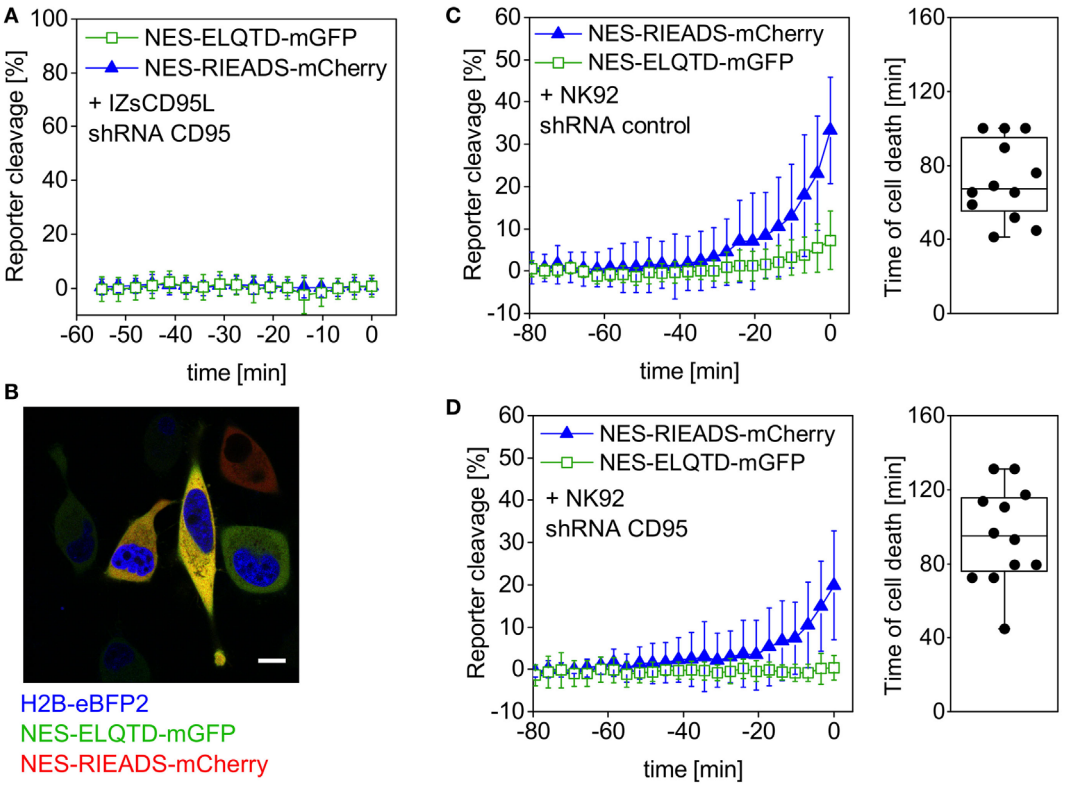

FIGURE 4 | Caspase-8 activity generated by NK92 cells is not induced by granzyme B. HeLa (CD48) cells were triple-transfected with NES-ELQTD-mGFP (for caspase-8) and NES-RIEADS-mCherry (for granzyme B) together with a plasmid encoding shRNA against CD95 and the fluorescent marker H2B-eBFP2 **(A,D)** or with a plasmid encoding control shRNA and H2B-eBFP2 **(C)**. **(A)** Cells expressing H2B-eBFP2 (and shRNA against CD95) and incubated with 1 µg/ml IZsCD95L neither showed reporter cleavage nor cell death. The plot shows data from 10 analyzed cells with time 0 being the end of the microscopy time series. **(B)** Field of view showing HeLa (CD48) cells imaged by confocal fluorescence microscopy. The image is an overlay of three fluorescence emission channels: the nuclear protein H2B-eBFP2 (blue) was expressed as fluorescent marker from the same plasmid encoding shRNA against CD95. NES-ELQTD-mGFP (green) and NES-RIEADS-mCherry (red) overlay result in yellow color depending on reporter amounts. Scale bar: 10 µm. **(C)** Cells expressing control shRNA and cocultured with NK92-C1 cells (E:T = 1) showed strong NES-RIEADS-mCherry reporter cleavage. The same cells showed on average up to 7% NES-ELQTD-mGFP reporter cleavage. **(D)** NES-ELQTD-mGFP reporter cleavage was absent in cells expressing shRNA against CD95, while granzyme B activity was clearly present in the same cells as seen from NES-RIEADS-mCherry reporter cleavage.

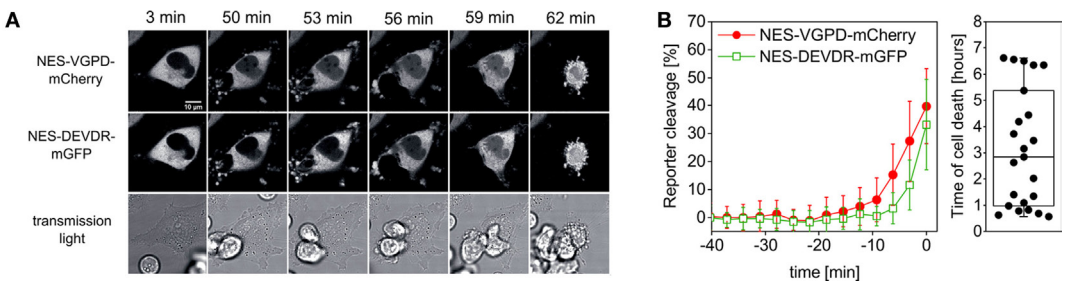

FIGURE 5 | Measurement of granzyme B and caspase-3 activity in single target cells. **(A,B)** HeLa cells transfected with CD48, NES-VGPD-mCherry (for granzyme B), and NES-DEVDR-mGFP (for caspase-3) were imaged by confocal microscopy upon incubation with NK92-C1 cells (E:T = 2). **(A)** Example images of the time series. Note that the fluorescence signal inside the nucleus is visible for NES-VGPD-mCherry at t = 50 min and for NES-DEVDR-mGFP at t = 56 min. Scale bar: 10 µm. **(B)** Quantification of reporter cleavage of 23 cells and boxplot showing the time of target cell death. On average, caspase-3 activity appears with a short delay of about 6 min after granzyme B activity.

example, on cyclic luciferase (29, 48), fluorophore quenching (31), FRET imaging (32, 33, 49), or subcellular localization of a fluorophore (34, 50). Our reporters provide us with the possibility to precisely investigate NK cell-induced cell death since they allow the measurement of two protease activities within the same cell. This feature is useful to correlate the

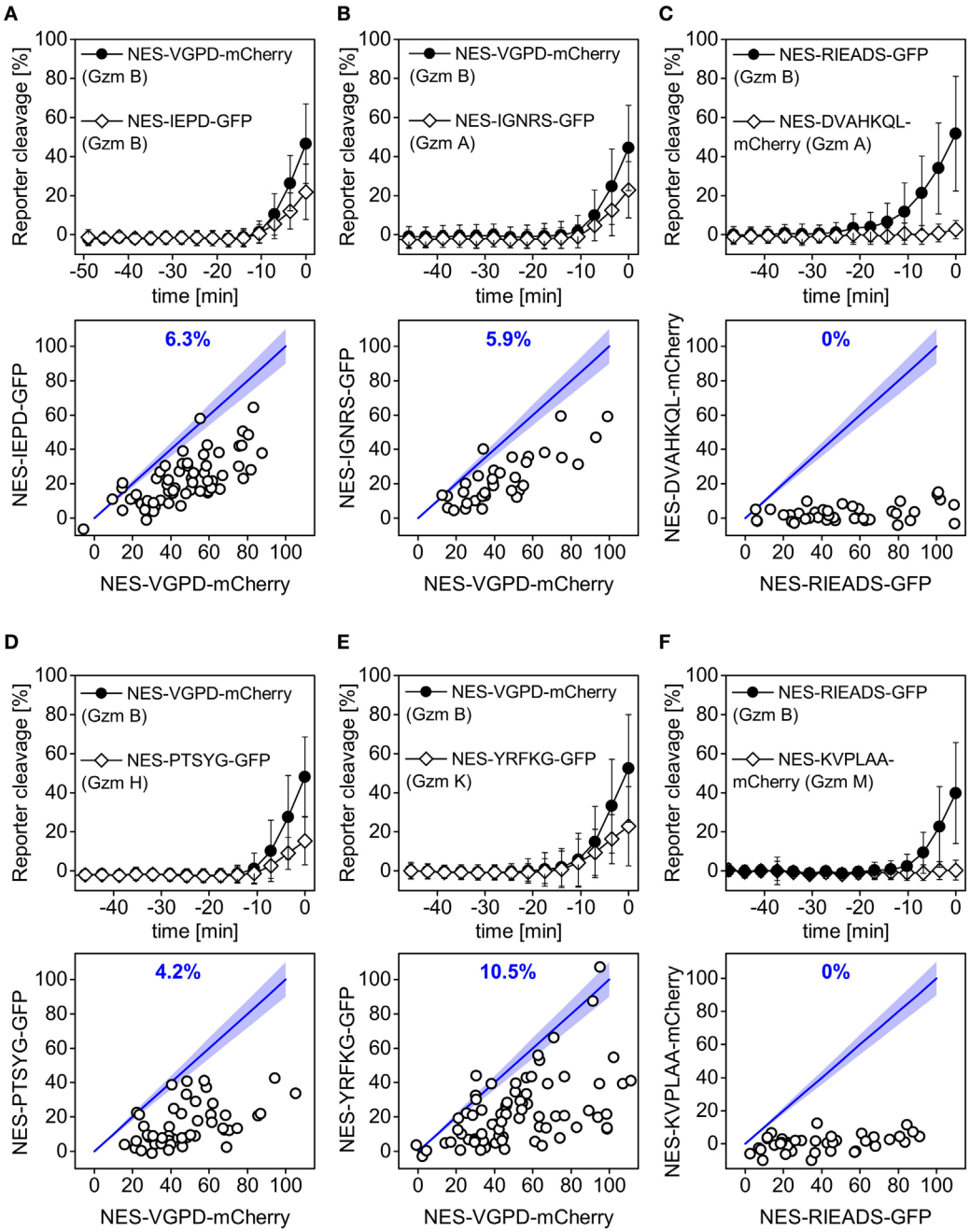

FIGURE 6 | Cleavage of reporters carrying the VGPD and RIEADS cleavage sites for granzyme B is predominant. Quantification of reporter cleavage upon NK92-C1 co-culture (E:T = 3) in HeLa (CD48) cells **(A,B,D,E)** or HeLa cells transfected with CD48 **(C,F)**, NES-VGPD-mCherry **(A,B,D,E)** or NES-RIEADS-GFP **(C,F)** and a second reporter, which was **(A)** NES-IEPD-GFP for granzyme B, **(B)** NES-IGNRS-GFP for granzyme A, **(C)** NES-DVAHKQL-mCherry for granzyme A, **(D)** NES-PTSYG-GFP for granzyme H, **(E)** NES-YRFKG-GFP for granzyme K, or **(F)** NES-KVPLAA-mCherry for granzyme M, with 34–82 cells per condition. Scatter plots below show reporter cleavage values in single cells at the measurement point before cell death. Percentages (blue) indicate the fraction of single cells showing more or equal (±10%) IEPD-, IGNRS-, DVAHKQL-, PTSYG-, YRFKG-, or KVPLAA-reporter cleavage compared to VGPD- and RIEADS-reporter cleavage.

activity of different enzymes within single cells and, therefore, independently of the large cell-to-cell variability due to the stochasticity of the NK–target cell contact. We used a confocal laser scanning microscope with a motorized stage that can record several user-defined fields of view one after the other. Thanks to that, we typically achieved the acquisition of around 40–50 single cells per experiment with a time-resolution of 2–4 min. The experimenter should find an optimal compromise between the number of imaged cells and the time resolution, which in turn depends on the speed of the autofocus and microscope type. In this context, a spinning disk microscope could provide higher imaging rate over a confocal laser scanning microscope.

Higher cell numbers per field of view may be also achieved by working with a target cell line that stably expresses the reporters. Regarding image analysis, we chose a simple manual workflow that we describe in detail in the Section "Materials and Methods," but we could also envision the development of automated image analysis workflows.

We demonstrate our approach using HeLa cells as targets as they are known to be responsive to death receptor ligands (34, 51) and granzymes (20, 27). Furthermore, adherent target cells such as HeLa cells are convenient for reporter expression and live microscopy. In particular, time-lapse microscopy of HeLa cells facilitates the identification of cell death, which was clearly visible from morphological changes like cell rounding, blebbing, and shrinkage. A limitation of the approach may be the use of target cells growing in suspension, as morphological changes due to cell death are not easily visible. We cannot exclude that one target cell was engaged by two or more NK cells at the same time, which may impact the kinetics of death signaling. Here, we worked with NK cell to target cell ratios in the range of 1/1 to 3/1. To ensure responses from single NK cells, we suggest as one possibility to add fewer NK cells, which should minimize the chance that several NK cells hit the same target cell.

We showed that the reporters developed here containing the RIEADS or the VGPD cleavage site are suitable for the measurement of granzyme B activity. We furthermore systematically tested putative reporters containing amino acid sequences that were previously shown to be cleaved by granzyme A, B, M, H, and K (39). Primary resting and activated NK cells were shown to express all granzymes, with the abundance order A, B > H > K, M (52). While granzyme B activity was the most prominent in our experiments, we could detect some activity of granzymes A, H, and K, but no activity of granzyme M. The reporters used here contain a nuclear export signal for the measurement of any enzyme activity in the cytosol. This may explain why the DVAHKQL reporter for granzyme A was not cleaved in target cells upon NK cell addition, since this substrate would naturally reside inside mitochondria (42). However, the contribution of other granzymes to cell death still remains to be further investigated, for example, by testing NK cells or CTLs at different maturation stages (53) or by taking into account the expression levels over long-term experiments (54).

Our experiments have demonstrated that granzyme B reporters can be applied in combination with caspase-8 or caspase-3 activity reporters. Strong caspase-3 activity correlated with granzyme B activity. These results support earlier studies (21, 23, 27, 28) showing that granzyme B can directly or indirectly (through BID) induce caspase-3 activation. Our data show that this is a fast process, with caspase-3 activity being detectable within 6 min after granzyme B activity. In contrast, caspase-8 activity was only detectable in target cells expressing the CD95 receptor but not in cells where CD95 was knocked-down, despite granzyme B activity. This suggests that there is no major activation of caspase-8 by granzyme B, in contrast to earlier studies (20). However, this also demonstrates that NK92 cells can indeed use two pathways to kill target cells: exocytosis of granzymes and perforin, resulting in detectable granzyme B activity inside the cytosol of target cells, and surface expression of CD95L and TRAIL, resulting in caspase-8 activity. Moreover, we also found clear reporter cleavage showing granzyme B and caspase-8 activity in HeLa and MDA-MB-468 breast carcinoma cells with activated primary NK cells as effector cells. This demonstrates the feasibility of the method for the study of different target cells and primary NK cells. Further work will be required to precisely understand how granzyme B and death receptor signaling are used by NK cells. We can envisage our reporters for the use in other target cells, where amounts of activating and inhibiting NK cell receptors are different or alternatively, where the amounts of death receptors or serpinB9 are different. Single-fluorescent protein reporters present a valuable tool to decipher cell death mechanisms induced by NK cells. We believe that this approach opens the door for the characterization of death receptor- versus granzyme-mediated target cell killing, in particular, the temporal evolution of these two death mechanisms in the context of serial killing by NK cells.

MATERIALS AND METHODS

Constructs

Human CD48 (UniProtKB P09326), human serpin B9/PI-9 (from Gateway cDNA library of the DKFZ), and IZ-sCD95L (55) were subcloned in the pIRES-puro2 vector. Fluorescent reporters were cloned based on constructs described previously (34) in pEGFP N1 and C1 vectors (Takara Bio Europe Clontech, Saint-Germain-en-Laye, France). DNA oligonucleotides encoding cleavage sites were cloned with AgeI/NotI or BsrGI/NotI (**Table 2**). The amino acid sequence starting from the N-terminus of the nuclear export signal (NES) is MNLVDLQKKLEELELDEQQ. shRNA against CD95 and scrambled shRNA (see **Table 2** for DNA sequences) were cloned in the pSilencer3.1 H1 Neo vector with HindIII and BamHI.

Cell Culture

HeLa and MDA-MB-468 cell lines were maintained in Dulbecco's modified eagle medium (Invitrogen, Darmstadt, Germany) containing 10% fetal calf serum (Biochrom AG, Berlin, Germany), penicillin/streptomycin, 100 µg/ml each (Invitrogen) and 1% non-essential amino acids plus 1 mM Sodium Pyruvate (Gibco) for MDA-MB-468 only. HeLa (CD48) cells over-express CD48 and were maintained in medium supplemented with 0.5 µg/ml puromycin (Sigma-Aldrich). NK92-C1 that stably express IL-2 were maintained in phenol red-free Minimum Essential Medium Eagle Alpha (MEMα, Sigma-Aldrich) without ribonucleosides and deoxyribonucleosides but containing sodium bicarbonate, supplemented with 2 mM L-glutamine, 50 µM 2-mercaptoethanol, 12.5% horse serum, 12.5% fetal bovine serum, and penicillin/streptomycin, 100 µg/ml each (Invitrogen). Human NK cells were isolated from PBMCs using the Dynabeads Untouched Human NK Cell kit (Thermo Fisher Scientific) according to the manufacturer's instructions. NK cells were between 90 and 99% CD3−, CD56+, and NKp46+ as assessed by flow cytometry. NK cells were expanded in 96-well round-bottom plates (Nunc) with irradiated K562-mbIL15-41BBL feeder cells (kind gift from Dario Campana) in IMDM Glutamax supplemented with 10% FCS and 1% penicillin, IL-2 (100 U/ml, NIH Cytokine Repository),

TABLE 2 | DNA sequence encoding protease cleavage sites used for plasmid cloning.

Cleavage site s: sense as: antisense	Oligonucleotide, 5′ → 3′
KVPLAA (s)	CCGGTGGCGGCAAGGTTCCACTTGCCGCCGG AGGAGGC
KVPLAA (as)	GGCCGCCTCCTCCGGCGGCAAGTGGAACCTT GCCGCCA
IEPDG (s)	CCGGTGGCGGCATTGAACCAGATGGTGGTGG AGGAGGC
IEPDG (as)	GGCCGCCTCCTCCACCACCATCTGGTTCAATG CCGCCA
IGNRS (s)	CCGGTGGCGGCATTGGTAACAGATCAGGTGGA GGAGGC
IGNRS (as)	GGCCGCCTCCTCCACCTGATCTGTTACCAATGC CGCCA
PTSYG (s)	CCGGTGGCGGCCCAACATCATATGGTGGTGGA GGAGGC
PTSYG (as)	GGCCGCCTCCTCCACCACCATATGATGTTGGGC CGCCA
YRFKG (s)	CCGGTGGCGGCTATCGCTTCAAGGGTGGTGGA GGAGGC
YRFKG (as)	GGCCGCCTCCTCCACCACCCTTGAAGCGATAG CCGCCA
DVAHKQL (s)	CCGGTGGCGGCGATGTTGCCCACAAGCAGCTT GGAGGAGGC
DVAHKQL (as)	GGCCGCCTCCTCCAAGCTGCTTGTGGGCAACA TCGCCGCCA
VGPDFGRG (s)	GTACAAGGGCGTAGGTGGCTCCGGTGGCGGAG TGGGACCCGACTTCGGAAGGGGCGGAGGAGGC
VGPDFGRG (as)	GGCCGCCTCCTCCGCCCCTTCCGAAGTCGGGT CCCACTCCGCCACCGGAGCCACCTACGCCCTT
RIEADS (s)	GTACAAGGGCGTAGGTGGCTCCGGTGGCGGAA GAATTGAAGCAGACTCAGGCGGAGGAGGC
RIEADS (as)	GGCCGCCTCCTCCGCCTGAGTCTGCTTCAATTC TTCCGCCACCGGAGCCACCTACGCCCTT
shRNA (CD95)	GATCCAGCGTATGACACATTGATTCTCAAGAGAA ATCAATGTGTCATACGCTTCTTTTTTGGAAA
shRNA (scrambled)	GATCCAATCTCATTCGATGCATACTTCAAGAGAGT ATGCATCGAATGAGATTCCTTTTTTGGAAA

and IL-15 (5 ng/ml, PAN-Biotech) at 37°C in a humidified 5% CO_2 incubator. IL-21 (100 ng/ml, Miltenyi Biotec) was added on the first day. Soluble CD95 ligand fused to the isoleucine-zipper domain (IZsCD95L, cloned in pIRES-puro2) was produced in 293T cells, which were seeded in 6-well plates. 24 h after cell transfection using JetPrime reagent (Polyplus), supernatant was replaced by fresh medium. At the next day, supernatant containing secreted ligand was harvested.

Microscopy

The presented approach uses fluorescence microscopy, which allows the extraction and correlation of several features, including the time of cell death. Time-lapse microscopy was performed with the TCS SP5 confocal laser scanning microscope from Leica (Leica Microsystems CMS GmbH, Mannheim, Germany) equipped with a 63×/1.4 OIL, HCX PL APO CS objective. We used the live data mode of the Leica software for autofocusing as described in Ref. (34). With the help of the autofocus option, the height position of the interface between the glass and the cell culture medium is found. From that position, an offset of a few micrometers was chosen to image a representative cross-section of the cell. We set the offset position so that an image of the cell is made approximately at the mid-height of the nucleus where the signal from the cytosol above and below the nucleus is minimal, and mostly cytosolic signal next to the nucleus is present. One image plane per field of view was acquired and cells were imaged once before the addition of NK cells. The resolution was 512 × 512 pixel and images were acquired in 8-bit or 16-bit. Fluorescence of mGFP and mCherry was acquired in line sequential mode. For mCherry, we used the helium–neon laser (561 nm), detection range: 600–660 nm, for mGFP, we used the argon laser (488 nm), detection range: 500–560 nm. Cells were grown and imaged in 8-well ibidi chambers (ibidi GmbH, Planegg/Martinsried, Germany). We applied one-, two-, or threefold more effector NK cells compared to target cells (E:T = 1, E:T = 2, or E:T = 3, respectively), hence about 6×10^4 to 1.8×10^5 NK cells per well. One field of view in confocal microscopy contained about 2 to 6 transfected cells. All cells expressing both reporters were analyzed. The time-resolution was about 2–4 min depending on the number of imaged fields and microscopy settings. Equal target cell preparation, equal NK cell preparation (cell number counting, transfection), and parallel measurement of different wells of an 8-well chamber allowed comparison of different conditions in one experiment. Time-series data were acquired for up to 12 h.

Image Analysis

Images were analyzed using ImageJ (56). To quantify the nuclear redistribution of fluorescence intensity over time in single cells, the nuclear intensity was measured. For this, images of each channel were background subtracted. To subtract the background, we selected a region of interest where no cell was present and applied the plugin for background subtraction, which we provided online https://github.com/jbeaudouin/NK_cell. Alternatively, we suggest using the background subtraction function in the "Process" tab provided in ImageJ or Fiji, which is based on the rolling ball algorithm. In most cases, two reporters were measured within one cell: to analyze them, one channel was assigned green, the other red, both were transformed into RGB, and they were then superimposed. The mean intensity within the nucleus was quantified by choosing a representative region within the nucleus at each time point until cell death was observed. We chose to normalize the nuclear intensity to the cytosolic intensity at each time point for soluble-cytosolic reporters to calculate the percentage of reporter cleavage.

The detailed image analysis workflow is as follows:

1. Open image stack of the first channel (time-series of one field of view) in ImageJ or Fiji. If applicable, open image stack of the second channel (time-series of one field of view) in

ImageJ or Fiji. At this stage, one works possibly with 8-bit or 16-bit—type images, depending on the microscope settings.
2. Subtract the background.
3. For two reporters measured: assign the stack with the channel of the first reporter in red (lookup table red), and the stack with the channel of the second reporter in green (for a third reporter, choose blue). At this stage, you still work with 8-bit or 16-bit—type images.
4. For two reporters measured: set the scale of the two stacks equal, meaning that the values in the 8-bit images would be set from 0 to 255, or values in the 16-bit images would be set from 0 to 65535.
5. Transform the stacks into RGB-type. Note that after this transformation, the intensity range is from 0 to 255.
6. Create an RGB-stack by adding the two stacks. For this use, the "Image Calculator" function in the "Process" tab of ImageJ or Fiji.
7. Save this stack.
8. Choose a region of interest using the rectangle or oval selection tool. Select a representative region within the nucleus or the cytosol, respectively.
9. Measure the mean signal of this selection using the plugin RGB_Measure3 (https://github.com/jbeaudouin/NK_cell). In the results table, a row containing three values for the mean intensity signal in the red channel, green channel, and the blue channel of the selected region of interest will be displayed. To call this plugin, please create a shortcut on the keyboard (Plugins tab > Shortcuts > Add shortcut)
10. Go to the next frame in the image stack with the help of another keyboard shortcut.
11. Alternate between workflow step 9 and 10 using the keyboard shortcuts and correct, if necessary, the position of the region of interest with the mouse cursor.
12. This procedure will give a table in the results window of ImageJ/Fiji, with each row being a time point measurement.
13. Copy this table in a program of your choice (Excel, Matlab, OriginLab) for further data analysis. Annotate the date of the experiment and experimental conditions.
14. The signal of the nucleus is then normalized (divided by), the signal measured in the cytosol, as explained in the first section of the results.
15. Despite the background subtraction, it may be useful to subtract a remaining offset. This signal may originate from signal in the nucleus at time 0 (before addition of NK cells).

Assessment of the Time of Target Cell Death

Cell death of HeLa target cells could be determined by the change of the cell's morphology. While cell rounding was often observed, we found also cells showing shrinkage without typical apoptotic blebbing. Changes in target cell morphology were unambiguously detected by monitoring living target cells by time-lapse microscopy in the fluorescence and transmission light channels.

Statistics

Data were visualized and analyzed using OriginLab software. Data groups were considered significantly different as indicated in the text, but considered not significantly different when P values were greater than 0.05 (ANOVA). Boxplots additionally show raw data points. Boxes indicate median, 25% quartile, and 75% quartile. Whiskers show minimal and maximal values. To plot the mean kinetics of reporter cleavage of single cell data, we set the time point that directly preceded cell death to time = 0 and calculated the mean and SD of single cell responses. The time values can, therefore, have a negative sign on the plots.

AUTHOR CONTRIBUTIONS

CL designed the study, performed experiments, analyzed the data, and wrote the paper. PS, IP, and DU performed experiments and analyzed data. MC isolated and purified primary human NK cells. RE, JB, and CW supervised the work and helped writing the paper.

ACKNOWLEDGMENTS

We kindly thank the DKFZ for providing the Gateway cDNA sequence of human serpin B9/PI-9. This work was supported by the Initiative and Networking Fund of the Helmholtz Association within the Helmholtz Alliance on Systems Biology/SBCancer. CW is supported by funding of the Leibniz Association (SAW-2013-IfADo-2) and the Deutsche Forschungsgemeinschaft (DFG, WA-1552/8-1). The publication of this article was funded by the Open Access Fund of the Leibniz Association.

SUPPLEMENTARY MATERIAL

The Supplementary Material for this article can be found online at https://www.frontiersin.org/articles/10.3389/fimmu.2018.01840/full#supplementary-material.

FIGURE S1 | Transient knockdown of CD95 in HeLa cells. HeLa cells were non transfected (black line) or transfected with a scrambled shRNA (blue line) or a shRNA against CD95 (red line). Cells were stained 3 days after transfection with or without the anti-CD95 antibody DX2.

FIGURE S2 | Granzyme B and caspase-8 activity in HeLa and MDA-MB-468 cells upon killing by primary natural killer (NK) cells. **(A)** HeLa-CD48 and **(B)** MDA-MB-468 cells were transfected with NES-ELQTD-mGFP (for caspase-8) and NES-VGPD-mCherry for granzyme B and incubated with activated primary human NK cells. Reporter cleavage was analyzed as described in **Figure 4**.

REFERENCES

1. Watzl C. How to trigger a killer: modulation of natural killer cell reactivity on many levels. *Adv Immunol* (2014) 124:137–70. doi:10.1016/B978-0-12-800147-9.00005-4
2. Mace EM, Dongre P, Hsu H-T, Sinha P, James AM, Mann SS, et al. Cell biological steps and checkpoints in accessing NK cell cytotoxicity. *Immunol Cell Biol* (2014) 92:245–55. doi:10.1038/icb.2013.96
3. Watzl C, Urlaub D, Fasbender F, Claus M. Natural killer cell regulation – beyond the receptors. *F1000Prime Rep* (2014) 6:87. doi:10.12703/P6-87

4. Ewen CL, Kane KP, Bleackley RC. A quarter century of granzymes. *Cell Death Differ* (2012) 19:28–35. doi:10.1038/cdd.2011.153
5. Strasser A, Jost PJ, Nagata S. The many roles of FAS receptor signaling in the immune system. *Immunity* (2009) 30:180–92. doi:10.1016/j.immuni.2009.01.001
6. Peter ME, Krammer PH. The CD95(APO-1/Fas) DISC and beyond. *Cell Death Differ* (2003) 10:26–35. doi:10.1038/sj.cdd.4401186
7. Stennicke HR, Jürgensmeier JM, Shin H, Deveraux Q, Wolf BB, Yang X, et al. Pro-caspase-3 is a major physiologic target of caspase-8. *J Biol Chem* (1998) 273:27084–90. doi:10.1074/jbc.273.42.27084
8. Barnhart BC, Alappat EC, Peter ME. The CD95 type I/Type II model. *Semin Immunol* (2003) 15:185–93. doi:10.1016/S1044-5323(03)00031-9
9. Wowk ME, Trapani JA. Cytotoxic activity of the lymphocyte toxin granzyme B. *Microbes Infect* (2004) 6:752–8. doi:10.1016/j.micinf.2004.03.008
10. Law RHP, Lukoyanova N, Voskoboinik I, Caradoc-Davies TT, Baran K, Dunstone MA, et al. The structural basis for membrane binding and pore formation by lymphocyte perforin. *Nature* (2010) 468:447–51. doi:10.1038/nature09518
11. Lopez JA, Jenkins MR, Rudd-Schmidt JA, Brennan AJ, Danne JC, Mannering SI, et al. Rapid and unidirectional perforin pore delivery at the cytotoxic immune synapse. *J Immunol* (2013) 191:2328–34. doi:10.4049/jimmunol.1301205
12. Lopez JA, Susanto O, Jenkins MR, Lukoyanova N, Sutton VR, Law RHP, et al. Perforin forms transient pores on the target cell plasma membrane to facilitate rapid access of granzymes during killer cell attack. *Blood* (2013) 121:2659–68. doi:10.1182/blood-2012-07-446146
13. Browne KA, Blink E, Sutton VR, Froelich CJ, Jans DA, Trapani JA. Cytosolic delivery of granzyme B by bacterial toxins: evidence that endosomal disruption, in addition to transmembrane pore formation, is an important function of perforin. *Mol Cell Biol* (1999) 19:8604–15. doi:10.1128/MCB.19.12.8604
14. Froelich CJ, Orth K, Turbov J, Seth P, Gottlieb R, Babior B, et al. New paradigm for lymphocyte granule-mediated cytotoxicity: target cells bind and internalize granzyme B, but an endosomolytic agent is necessary for cytosolic delivery and subsequent apoptosis. *J Biol Chem* (1996) 271:29073–9. doi:10.1074/jbc.271.46.29073
15. Thiery J, Keefe D, Saffarian S, Martinvalet D, Walch M, Boucrot E, et al. Perforin activates clathrin- and dynamin-dependent endocytosis, which is required for plasma membrane repair and delivery of granzyme B for granzyme-mediated apoptosis. *Blood* (2010) 115:1582–93. doi:10.1182/blood-2009-10-246116
16. Bots M, Medema JP. Granzymes at a glance. *J Cell Sci* (2006) 119:5011–4. doi:10.1242/jcs.03239
17. Joeckel LT, Bird PI. Are all granzymes cytotoxic in vivo? *Biol Chem* (2014) 395:181–202. doi:10.1515/hsz-2013-0238
18. Susanto O, Trapani JA, Brasacchio D. Controversies in granzyme biology. *Tissue Antigens* (2012) 80:477–87. doi:10.1111/tan.12014
19. Li H, Zhu H, Xu CJ, Yuan J. Cleavage of BID by caspase 8 mediates the mitochondrial damage in the Fas pathway of apoptosis. *Cell* (1998) 94:491–501. doi:10.1016/S0092-8674(00)81590-1
20. Medema JP, Toes REM, Scaffidi C, Zheng TS, Flavell RA, Melief CJM, et al. Cleavage of FLICE (caspase-8) by granzyme B during cytotoxic T lymphocyte-induced apoptosis. *Eur J Immunol* (1997) 27:3492–8. doi:10.1002/eji.1830271250
21. Quan LT, Tewari M, O'Rourke K, Dixit V, Snipas SJ, Poirier GG, et al. Proteolytic activation of the cell death protease Yama/CPP32 by granzyme B. *Proc Natl Acad Sci U S A* (1996) 93:1972–6. doi:10.1073/pnas.93.5.1972
22. Yang X, Stennicke HR, Wang B, Green DR, Jänicke RU, Srinivasan A, et al. Granzyme B mimics apical caspases: description of a unified pathway for trans-activation of executioner caspase-3 and -7. *J Biol Chem* (1998) 273:34278–83. doi:10.1074/jbc.273.51.34278
23. Andrade F, Roy S, Nicholson D, Thornberry N, Rosen A, Casciola-Rosen L. Granzyme B directly and efficiently cleaves several downstream caspases substrates: Implications for CTL-induced apoptosis. *Immunity* (1998) 8:451–60. doi:10.1016/S1074-7613(00)80550-6
24. Atkinson EA, Barry M, Darmon AJ, Shostak I, Turner PC, Moyer RW, et al. Cytotoxic T lymphocyte-assisted suicide: caspase 3 activation is primarily the result of the direct action of granzyme B. *J Biol Chem* (1998) 273:21261–6. doi:10.1074/jbc.273.33.21261
25. Goping IS, Barry M, Liston P, Sawchuk T, Constantinescu G, Michalak KM, et al. Granzyme B-induced apoptosis requires both direct caspase activation and relief of caspase inhibition. *Immunity* (2003) 18:355–65. doi:10.1016/S1074-7613(03)00032-3
26. Barry M, Heibein JA, Pinkoski MJ, Lee SF, Moyer RW, Green DR, et al. Granzyme B short-circuits the need for caspase 8 activity during granule-mediated cytotoxic T-lymphocyte killing by directly cleaving Bid. *Mol Cell Biol* (2000) 20:3781–94. doi:10.1128/MCB.20.11.3781-3794.2000
27. Pinkoski MJ, Waterhouse NJ, Heibein JA, Wolf BB, Kuwana T, Goldstein JC, et al. Granzyme B-mediated apoptosis proceeds predominantly through a Bcl-2-inhibitable mitochondrial pathway. *J Biol Chem* (2001) 276:12060–7. doi:10.1074/jbc.M009038200
28. Sutton VR, Davis JE, Cancilla M, Johnstone RW, Ruefli AA, Sedelies K, et al. Initiation of apoptosis by granzyme B requires direct cleavage of bid, but not direct granzyme B-mediated caspase activation. *J Exp Med* (2000) 192:1403–14. doi:10.1084/jem.192.10.1403
29. Li J, Figueira SK, Vrazo ACA, Binkowski BF, Butler BL, Tabata Y, et al. Real-time detection of CTL function reveals distinct patterns of caspase activation mediated by Fas versus granzyme B. *J Immunol* (2014) 193:519–28. doi:10.4049/jimmunol.1301668
30. Vrazo AC, Hontz AE, Figueira SK, Butler BL, Ferrell JM, Binkowski BF, et al. Live cell evaluation of granzyme delivery and death receptor signaling in tumor cells targeted by human natural killer cells. *Blood* (2015) 126:e1–10. doi:10.1182/blood-2015-03-632273
31. Packard BZ, Telford WG, Komoriya A, Henkart PA. Granzyme B activity in target cells detects attack by cytotoxic lymphocytes. *J Immunol* (2007) 179:3812–20. doi:10.4049/jimmunol.179.6.3812
32. Choi PJ, Mitchison TJ. Imaging burst kinetics and spatial coordination during serial killing by single natural killer cells. *Proc Natl Acad Sci U S A* (2013) 110:6488–93. doi:10.1073/pnas.1221312110
33. Zhu Y, Huang B, Shi J, Zhu Y, Huang B, Shi J. Fas ligand and lytic granule differentially control cytotoxic dynamics of natural killer cell against cancer target. *Oncotarget* (2016) 7(30):5. doi:10.18632/oncotarget.9980
34. Beaudouin J, Liesche C, Aschenbrenner S, Hörner M, Eils R. Caspase-8 cleaves its substrates from the plasma membrane upon CD95-induced apoptosis. *Cell Death Differ* (2013) 20:1–12. doi:10.1038/cdd.2012.156
35. Backes C, Kuentzer J, Lenhof HP, Comtesse N, Meese E. GraBCas: a bioinformatics tool for score-based prediction of Caspase- and granzyme B-cleavage sites in protein sequences. *Nucleic Acids Res* (2005) 33:208–13. doi:10.1093/nar/gki433
36. Casciola-Rosen L, Garcia-Calvo M, Bull HG, Becker JW, Hines T, Thornberry NA, et al. Mouse and human granzyme B have distinct tetrapeptide specificities and abilities to recruit the bid pathway. *J Biol Chem* (2007) 282:4545–52. doi:10.1074/jbc.M606564200
37. Fischer U, Stroh C, Schulze-Osthoff K. Unique and overlapping substrate specificities of caspase-8 and caspase-10. *Oncogene* (2006) 25:152–9. doi:10.1038/sj.onc.1209015
38. McStay GP, Salvesen GS, Green DR. Overlapping cleavage motif selectivity of caspases: implications for analysis of apoptotic pathways. *Cell Death Differ* (2008) 15:322–31. doi:10.1038/sj.cdd.4402260
39. Mahrus S, Craik CS. Selective chemical functional probes of granzymes A and B reveal granzyme B is a major effector of natural killer cell-mediated lysis of target cells. *Chem Biol* (2005) 12:567–77. doi:10.1016/j.chembiol.2005.03.006
40. Guo Y, Chen J, Shi L, Fan Z. Valosin-containing protein cleavage by granzyme K accelerates an endoplasmic reticulum stress leading to caspase-independent cytotoxicity of target tumor cells. *J Immunol* (2010) 185:5348–59. doi:10.4049/jimmunol.0903792
41. Mahrus S, Kisiel W, Craik CS. Granzyme M is a regulatory protease that inactivates proteinase inhibitor 9, an endogenous inhibitor of granzyme B. *J Biol Chem* (2004) 279:54275–82. doi:10.1074/jbc.M411482200
42. Martinvalet D, Dykxhoorn DM, Ferrini R, Lieberman J. Granzyme A cleaves a mitochondrial complex I protein to initiate caspase-independent cell death. *Cell* (2008) 133:681–92. doi:10.1016/j.cell.2008.03.032
43. Hoffmann SC, Cohnen A, Ludwig T, Watzl C. 2B4 engagement mediates rapid LFA-1 and actin-dependent NK cell adhesion to tumor cells as measured by single cell force spectroscopy. *J Immunol* (2011) 186:2757–64. doi:10.4049/jimmunol.1002867
44. Kaiserman D, Bird PI. Control of granzymes by serpins. *Cell Death Differ* (2010) 17:586–95. doi:10.1038/cdd.2009.169

45. Bratke K, Kuepper M, Bade B, Virchow JC, Luttmann W. Differential expression of human granzymes A, B, and K in natural killer cells and during CD8+ T cell differentiation in peripheral blood. *Eur J Immunol* (2005) 35:2608–16. doi:10.1002/eji.200526122
46. Grossman WJ, Verbsky JW, Tollefsen BL, Kemper C, Atkinson JP, Ley TJ. Differential expression of granzymes A and B in human cytotoxic lymphocyte subsets and T regulatory cells. *Blood* (2004) 104:2840–8. doi:10.1182/blood-2004-03-0859
47. Krzewski K, Coligan JE. Human NK cell lytic granules and regulation of their exocytosis. *Front Immunol* (2012) 3:335. doi:10.3389/fimmu.2012.00335
48. Kanno A, Yamanaka Y, Hirano H, Umezawa Y, Ozawa T. Cyclic luciferase for real-time sensing of caspase-3 activities in living mammals. *Angew Chem Int Ed Engl* (2007) 46:7595–9. doi:10.1002/anie.200700538
49. Rehm M, Parsons MJ, Bouchier-Hayes L. Measuring caspase activity by Förster resonance energy transfer. *Cold Spring Harb Protoc* (2015) 2015: db.rot082560. doi:10.1101/pdb.prot082560
50. Lin S-Y, Chen N-T, Sun S-P, Chang JC, Wang Y-C, Yang C-S, et al. The protease-mediated nucleus shuttles of subnanometer gold quantum dots for real-time monitoring of apoptotic cell death. *J Am Chem Soc* (2010) 132:8309–15. doi:10.1021/ja100561k
51. Albeck JG, Burke JM, Aldridge BB, Zhang M, Lauffenburger DA, Sorger PK. Quantitative analysis of pathways controlling extrinsic apoptosis in single cells. *Mol Cell* (2008) 30:11–25. doi:10.1016/j.molcel.2008.02.012
52. Rieckmann JC, Geiger R, Hornburg D, Wolf T, Kveler K, Jarrossay D, et al. Social network architecture of human immune cells unveiled by quantitative proteomics. *Nat Immunol* (2017) 18:583–93. doi:10.1038/ni.3693
53. Nakazawa T, Agematsu K, Yabuhara A. Later development of Fas ligand-mediated cytotoxicity as compared with granule-mediated cytotoxicity during the maturation of natural killer cells. *Immunology* (1997) 92:180–7. doi:10.1046/j.1365-2567.1997.00343.x
54. Meiraz A, Garber OG, Harari S, Hassin D, Berke G. Switch from perforin-expressing to perforin-deficient CD8+ T cells accounts for two distinct types of effector cytotoxic T lymphocytes in vivo. *Immunology* (2009) 128:69–82. doi:10.1111/j.1365-2567.2009.03072.x
55. Walczak H, Miller RE, Ariail K, Gliniak B, Griffith TS, Kubin M, et al. Tumoricidal activity of tumor necrosis factor-related apoptosis-inducing ligand in vivo. *Nat Med* (1999) 5:157–63. doi:10.1038/5517
56. Schneider CA, Rasband WS, Eliceiri KW. NIH Image to ImageJ: 25 years of image analysis. *Nat Methods* (2012) 9:671–5. doi:10.1038/nmeth.2089

Conflict of Interest Statement: The authors declare that the research was conducted in the absence of any commercial or financial relationships that could be construed as a potential conflict of interest.